

Peak effect in optimally doped p -type single-crystal $\text{Ba}_{0.5}\text{K}_{0.5}\text{Fe}_2\text{As}_2$ studied by ac magnetization measurements

J. Ge,^{1,*} J. Gutierrez,¹ J. Li,^{1,2} J. Yuan,² H.-B. Wang,^{2,3} K. Yamaura,^{2,4} E. Takayama-Muromachi,^{4,5} and V. V. Moshchalkov¹

¹*INPAC—Institute for Nanoscale Physics and Chemistry, KU Leuven, Celestijnenlaan 200D, B-3001 Leuven, Belgium*

²*Superconducting Properties Unit, National Institute for Materials Science, 1-1 Namiki, Tsukuba, Ibaraki 305-0044, Japan*

³*Research Institute of Superconductor Electronics, Nanjing University, Nanjing 210093, China*

⁴*Graduate School of Chemical Sciences and Engineering, Hokkaido University, Sapporo, Hokkaido 060-0810, Japan*

⁵*International Center for Materials Nanoarchitectonics (WPI-MANA), National Institute for Materials Science, 1-1 Namiki, Tsukuba, Ibaraki 305-0044, Japan*

(Received 28 August 2013; revised manuscript received 2 October 2013; published 14 October 2013)

We have used the ac magnetic susceptibility to investigate the vortex state in an optimally doped p -type $\text{Ba}_{0.5}\text{K}_{0.5}\text{Fe}_2\text{As}_2$ single crystal under various ac and dc fields. A peak effect is observed in the temperature dependence of the in-phase ac susceptibility, indicating an order-disorder transition on the vortex phase diagram. The peak effect displays an anomalous history effect compared with other type-II superconductors, which we ascribe to the strong pinning existing in the material. We observe the development of a small dissipation peak at the temperature T_{p2} slightly below the peak effect region. Similar to the peak effect boundary, T_{p2} delimits a region in the H - T phase diagram which is independent on the ac field amplitude. We argue that this small peak may arise from the softening of the vortex lattice, leading to a collective pinning of the whole vortex lattice. This effect assists and further enhances the peak effect occurring in the $\text{Ba}_{0.5}\text{K}_{0.5}\text{Fe}_2\text{As}_2$ superconductor.

DOI: [10.1103/PhysRevB.88.144505](https://doi.org/10.1103/PhysRevB.88.144505)

PACS number(s): 64.60.Cn, 74.25.Dw, 74.25.Ha, 74.70.Xa

I. INTRODUCTION

In both low and high T_c superconductors, one of the most interesting phenomena in the Abrikosov vortex state of type-II superconductors is the nonmonotonous dependence of the critical current J_c on temperature or/and magnetic field, which is well known as the peak effect (PE).¹ Among all possible explanations, it has been recently proposed that the transition from a quasicrystalline Bragg glass with weak random pinning to a disordered phase with strong pinning is the responsible for the peak effect.^{2–5} The study of the PE holds the key to help us gaining insight in the subjects of vortex matter and its dynamics in superconductors, as well as in order-disorder transition phenomena which are found in a wide range of materials and may have a significant impact on their properties.

The discovery of high temperature superconductivity in iron-based superconductors has attracted extensive interest of the researchers.⁶ The high upper critical field (H_{c2}),⁷ high critical current density (J_c), and relatively low anisotropy⁸ favor future potential applications. The new high T_c superconductors also provide a promising route to unveil the puzzling questions remaining for other superconducting systems. Normally the PE is observed only in high quality single crystals, since in such materials it is expected that there is a small number of defects working as strong pinning centers. In such systems the remaining pointlike defects such as vacancies may play an important role for the occurrence of the PE.⁹ However, the iron-based superconductors have been reported to exhibit very strong pinning strength especially in the so called 122 phase (e.g., $\text{A}_{1-x}\text{M}_x\text{Fe}_2\text{As}_2$, A = alkaline-earth element, M = alkaline metal), where the effective pinning potential reaches a record high value.¹⁰ The vortex configuration in samples with strong intrinsic pinning is more disordered than in a sample with weaker pinning. Highly inhomogeneous vortex patterns have been reported in 122 family compounds^{11–13}

and other iron-based superconductors.^{14,15} Whether the vortex matter order-disorder transition still exists in iron-based superconductors remains an open question.

There are many different ways to reveal the PE, such as isothermal magnetization, electrical transport, and ac susceptibility measurements. In isothermal magnetization measurements J_c , deduced from the magnetization hysteresis loops, increases with the magnetic field after the first peak of the penetration field, which is also called fishtail effect or second magnetization peak (SMP). However, it has been found that in some superconductors the temperature derived from SMP is not consistent with the peak effect from electrical transport measurements. There might be a different mechanism behind these two phenomena.¹⁶ In standard electrical transport measurements, vortices undergo some type of current induced reorganization, and therefore the original vortex lattice configuration is not accessible. In that sense, the ac susceptibility technique can be regarded as a special electrical transport experiment, where the in-phase component probes the shielding supercurrents and the out-of phase component measures the energy dissipation due to the vortex motion. Moreover, the higher harmonics of ac susceptibility also allow us to study the nonlinear response of the vortex lattice.^{17,18} Compared with the electrical transport and isothermal magnetization measurements, the ac susceptibility technique has the advantage of acquiring information in a much shorter time window (10^{-5} – 10^{-1} s)^{19,20} which is important in the study of vortex order-disorder transitions.

Until now the SMP have been reported from isothermal magnetization measurements in many kinds of iron-based superconductors^{21,22} and most of them are attributed to the crossover from the elastic to the plastic pinning. However, no PE has been observed either by electrical transport or by ac susceptibility measurements.

In this paper we report the observation of the PE in an optimally doped *p*-type $\text{Ba}_{0.5}\text{K}_{0.5}\text{Fe}_2\text{As}_2$ superconductor through ac susceptibility measurements. A history effect in the PE regime is studied which might arise from the strong intrinsic pinning in $\text{Ba}_{0.5}\text{K}_{0.5}\text{Fe}_2\text{As}_2$. By mapping out the PE phase diagram, we found an enhanced disordered regime with strong pinning due to increase of the shaking field.

II. EXPERIMENTS

The studied single crystal $\text{Ba}_{0.5}\text{K}_{0.5}\text{Fe}_2\text{As}_2$ was prepared using a high-pressure technique as been reported in Ref. 23. Compared with the normal preparation method, the high-pressure technique provides the highest quality single crystals. The sample, with sizes of $\sim 1 \times 1.3 \times 0.5 \text{ mm}^3$, is characterized by a $T_c = 38.2 \text{ K}$ and $\Delta T_c = 0.4 \text{ K}$ (10%–90% criterion). The ac susceptibility measurements were performed using a Quantum Design PPMS with an external dc field up to 9 T and an ac field with an amplitude range of $h_{ac} = 0.2\text{--}12 \text{ Oe}$. Both dc and ac fields are perpendicular to the sample surface (*ab* plane) in all the measurements.

III. RESULTS AND DISCUSSION

Figure 1 shows the in-phase $\chi'(T)$ and the out-of-phase $\chi''(T)$ ac susceptibility as a function of temperature and dc magnetic field. The in-phase signal is related to the shielding capabilities of the sample, and at low dc fields the $\chi'(T)$ exhibits a steplike diamagnetic response just below T_c , indicating the onset of superconductivity. Similarly, the

out-of-phase signal arises due to the dissipative ac losses within the superconductor. $\chi''(T)$ displays an obvious peak at the temperature T_{irr} coinciding with the drop in $\chi'(T)$, this peak signals the onset of dissipation caused by the vortex motion close to T_c due to the melting of the vortex glass. Therefore, T_{irr} is usually defined as the crossover between a glass phase (irreversible magnetization) and a liquid phase (reversible magnetization).^{24–26} With increasing dc field, both T_c and T_{irr} shift to lower temperatures. Above the threshold field $H_{thr} = 0.3 \text{ T}$, a kink at the temperature T_{peak} starts to develop on the in-phase curve [Fig. 1(c)], at the same time, on the out-of-phase curve a corresponding dip emerges with a broad peak appearing at temperature of T_{p3} [Fig. 1(d)]. With further increasing fields, the kink on the $\chi'(T)$ curve becomes more pronounced and gradually transforms into a distinct dip, which is well known as the peak effect.^{4,27,28}

It is clear from Fig. 1(a) that there exists an area around T_{peak} with higher shielding compared with the area around T_{onset} and below. Correspondingly, in Fig. 1(b), around the same area the vortex lattice exhibits lower dissipation, there indicates a stronger pinning in that temperature regime. It has been proposed that T_{onset} (the onset of the PE) signals the crossover from an ordered-weak pinning vortex phase to a disordered-strong pinning vortex phase.^{2–4} It is worth noticing that the broad peak occurring in χ'' , which emerges at T_{p3} , was also observed in high T_c cuprates, where it is believed to be a signal for the onset of weak bulk pinning when vortices form a lattice.²⁶ We have identified that the threshold field (H_{thr}) above which the PE appears depends on the amplitude of the shaking field h_{ac} . A similar effect has also been observed in other superconductors such as MgB_2 ,²⁸ Nb ,²⁹ and binary alloy V-21 at. %Ti.⁴ The reason why the PE only appears above H_{thr} is still unclear. It has been suggested that the appearance of a PE in a type-II superconductor may be correlated with a multicritical point (MCP) on the vortex phase diagram where the third critical field, upper critical field, and PE boundaries meet at the same point.²⁹ In our crystal, no sign of surface superconductivity is observed. However, we do observe that below H_{thr} the out-of-phase peak height at T_{irr} decreases with increasing dc field, while above it, $\chi''(T_{irr})$ increases with the field. The field dependence of $\chi''(T_{irr})$ is displayed in the inset of Fig. 1(b), from which the H_{thr} can be defined as the curve's minimum. Although the mechanism behind it is still not clear, the same behavior for χ'' has been reported in $\text{YBa}_2\text{Cu}_3\text{O}_7$.²⁶ We suggest that the decrease of $\chi''(T)$ with increasing H_{dc} might be due to the precursor of the PE where strong pinning evolves. This might provide an easier way to estimate the H_{thr} compared with the progressive emergence of PE on the in-phase curves.

The PE often shows metastability and history effects in both low and high- T_c superconductors when measuring by using different thermomagnetic processes.^{16,27,30,31} Figure 2 plots the in-phase ac susceptibility data obtained in different measuring processes: (1) field-cooled cooling down (FCC), (2) field-cooled warming up (FCW-#), where # is the temperature to which the sample has been cooled down, and (3) field-cooled warming up after cooling with the ac field on (FCW-ac). It is clearly observed that above the characteristic temperature T^* , as indicated by the dashed line, all the curves merge while below T^* , χ' displays a strong history effect, with T_{peak}

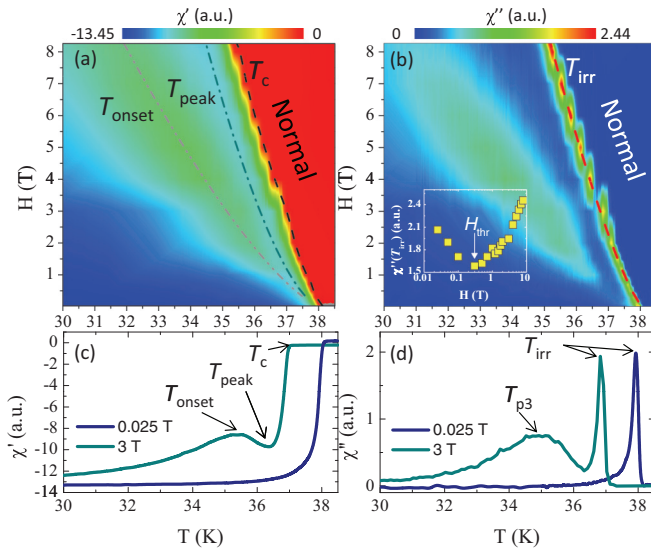


FIG. 1. (Color online) (a) In-phase and (b) out-of-phase of the ac susceptibility as a function of temperature and dc magnetic field. The bright red color (dark blue) in (a) and (b) indicates low (high) shielding of the magnetic field and high (low) dissipation of the vortex lattice, respectively. (c) and (d) present the typical curves of the $\chi'(T)$ and $\chi''(T)$ measured below and above the threshold field H_{thr} , respectively. All the measurements were done through field-cooling process with $h_{ac} = 1 \text{ Oe}$ at $f = 1333 \text{ Hz}$. The inset shows the $\chi''(T_{irr})$ value as a function of magnetic field, where H_{thr} is defined as the minimum of $\chi''(T_{irr})$ at $H = 0.3 \text{ T}$. The lines in (a) and (b) indicate the positions of T_c , T_{onset} , T_{peak} , and T_{irr} .

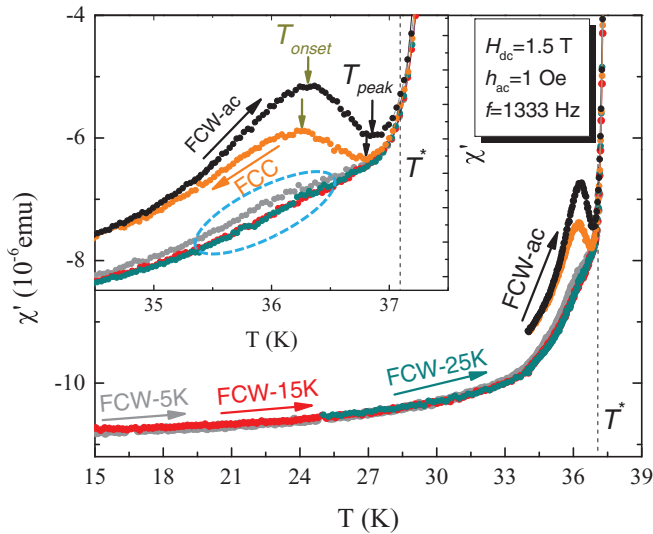


FIG. 2. (Color online) In-phase of the ac susceptibility recorded in various cooling and warming processes at $H_{dc} = 1.5$ T and $h_{ac} = 1$ Oe. Inset shows the enlargement of the main panel at the peak effect region. The arrows show the direction of temperature variation. The vertical arrows show the position of T_p^{on} and T_{peak} . The dashed circles indicate the kink of FCW-5 K curve in the PE region due to low temperature spontaneous ordering.

and T_{onset} slightly depending on the magnetic history. When performing FCW from low temperatures, the χ' curves exhibit very weak PE (FCW-5 K) or even no trace of PE (FCW-15 K and FCW-25 K). As the PE is a signature of an order-disorder transition, the disappearing of the PE through field cooling in the absence of an ac field indicates that the vortex lattice remains in a metastable disordered and strongly pinned configuration. Contrary to what have been reported in FCW experiments in a conventional superconductor NbSe₂,²⁷ where a spontaneous ordering occurs at low temperature; the overlap of FCW-15 K and FCW-25 K curves might arise from the strong intrinsic pinning in Ba_{0.5}K_{0.5}Fe₂As₂ single crystals.³² As illustrated by the inset of Fig. 2, only at low enough temperatures (FCW-5 K), the elastic force between vortices can partially overcome the interaction between vortices and pinning potentials, reconfiguring the vortex lattice into a more ordered state. Indeed, the FCW-5 K curve does exhibit a small peak and slight kink around the PE region, which may hint towards a spontaneous ordering of vortex lattice at low enough temperatures. In the Ba_{0.5}K_{0.5}Fe₂As₂ single crystal superconductor we find that the most ordered state is obtained by performing a FCW with an ac field on (FCW-ac), as demonstrated by the black circles in Fig. 2. This is reasonable since in the nonlinear regime (close to T_c), when cooling with and ac field on, the vortex lattice experiences a transition towards a more ordered (lower pinning) configuration as displayed by the FCC curve. Following this path, the system warms up (FCW-ac) in a lower pinning potential as compared to the FCW-# experiments. Therefore, the hysteresis displayed by the FCC and FCW-ac curves supports the hypothesis of a spontaneous vortex lattice reordering occurring as the temperature is decreased. When the vortex lattice is cooled under a reduced pinning landscape (FCC), the elastic vortex-vortex interaction is able to overcome the vortex pinning

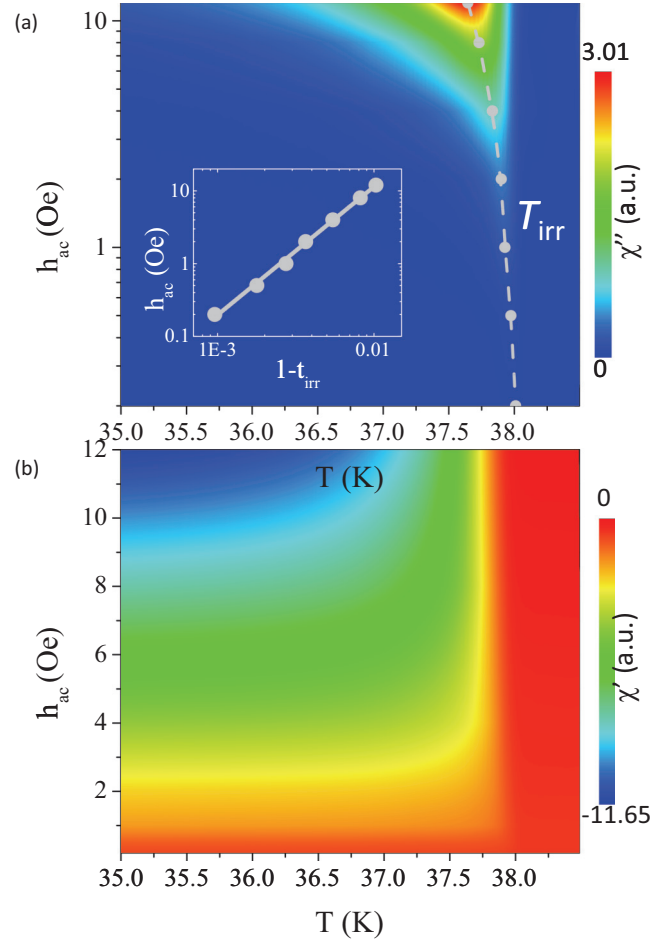


FIG. 3. (Color online) Contour plot of the (a) out-of-phase and (b) in-phase of the ac susceptibility as a function of temperature, for h_{ac} varying from 0.2 to 12 Oe ($f = 1333$ Hz) at $H_{dc} = 0.025$ T. Inset shows the log-log plot of h_{ac} vs $(1 - t_{irr})$, where $t_{irr} = T/T_c$.

interaction further reordering the lattice, the fact that shows up on the FCW-ac curve as an enhanced PE. Since the thermomagnetic history plays an important role in determining the PE and mapping out the vortex matter phase diagram, for the remaining of the paper we concentrate on the FCC measurements for mutual comparisons of the ac susceptibility.

As discussed above, there exists a threshold field H_{thr} above which the PE appears. We have studied if there is any difference in vortex behavior above and below H_{thr} . Figure 3 presents the ac susceptibility as a function of the temperature at $H_{dc} = 0.025$ T and h_{ac} varying from 0.2 to 12 Oe. No PE is observed even at $h_{ac} = 12$ Oe. With increasing h_{ac} , the low temperature part of χ' shifts downward corresponding to an increase in the screening current. At the same time, the χ'' peak becomes broader, shifts to lower temperature, and its height increases. All these features support a scenario of nonlinear response of the sample, which is well predicted by the critical state model.³³ It has been proposed within the Ginzburg-Landau theory and the collective pinning activation energy framework³⁴ that, at constant dc field ($H_{dc} \gg h_{ac}$) and frequency, the $\ln(h_{ac})$ follows a straight line dependence with $\ln(1 - t_{irr})$ with slope of q/μ , where $t_{irr} = T_{irr}/T_c$. We have chosen $q = 3/2$ as in most high T_c superconductors³⁴⁻³⁶ and

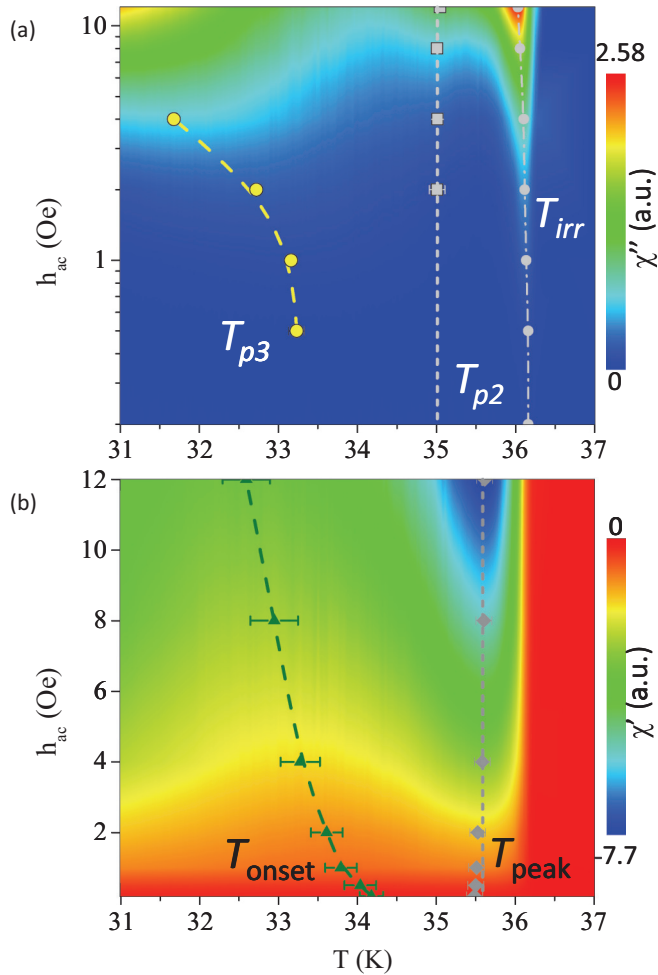


FIG. 4. (Color online) Contour plot of the temperature dependence of (a) out-of-phase and (b) in-phase of the ac susceptibility for various ac fields at $H_{dc} = 5$ T, $f = 1333$ Hz. The dashed and short dashed lines in both panels mark the positions of T_{p3} , T_{p2} , T_{onset} , and T_{peak} , respectively.

fullerene superconductors,³⁷ and μ is the glassy exponent of the collective pinning theory. According to it, the current density dependent activation energy can be written as $U(J) = U_0(T, B)(J_{c0}/J)^\mu$, where $\mu = 1/7$, $3/2$, and $7/9$ for a single vortex, small bundles, and large bundles, respectively. For our $\text{Ba}_{0.5}\text{K}_{0.5}\text{Fe}_2\text{As}_2$ single crystal the log-log plot of h_{ac} and $(1 - t_{irr})$ [inset to Fig. 3(a)] gives a slope of 1.7, indicating that the major pinning mechanism is due to large bundles. We have performed the same analysis of the data at $H_{dc} = 5$ T [Fig. 4(a)] which yields a slope of 1.5, again pointing towards bundle vortex pinning as the major contribution. These values are in the same range as those found for the YBCO films,³⁸ thus supporting the high pinning scenario for $\text{Ba}_{0.5}\text{K}_{0.5}\text{Fe}_2\text{As}_2$ crystals.

Figure 4 presents the temperature dependence of the ac susceptibility for different h_{ac} at $f = 1333$ Hz and $H_{dc} = 5$ T. From the in-phase part we see the PE is well formed even at $h_{ac} = 0.2$ Oe. With increasing the amplitude of the ac field, T_{peak} remains unchanged while T_{onset} , the temperature at which χ' exhibits a maximum, moves to lower temperature as

indicated by the dashed lines in Fig. 4(b). Within the order-disorder phenomenological interpretation of the peak effect, although T_{onset} does not signal the phase transition, it marks the point where the disordered phase percolates and topological defects start to proliferate. The slight shift of T_{onset} towards lower temperatures as h_{ac} increases occurs due to the enhanced penetration of Meissner currents into the sample for higher h_{ac} fields.

From analyzing the out-of phase curves at high dc magnetic fields [Fig. 4(a)] we observe that above $h_{ac} = 2$ Oe a small peak appears at T_{p2} , just below the temperature T_{peak} . The corresponding peak value becomes more and more pronounced as h_{ac} increases, while the temperature T_{p2} , at which the peak appears, is independent on h_{ac} . The small peak was also observed in both $\text{YBa}_2\text{Cu}_3\text{O}_7$ ²⁶ and NbSe_2 ,²⁷ and it was suggested that it arises due to vortex lattice softening and synchronous trapping of vortices.²⁶ To further investigate the role of the second peak, in Figs. 5(a)–5(d) we present the in-phase and out-of-phase ac susceptibility, and the derivative $d\chi'(T)/dT$ (open circles) for various dc fields at $f = 1333$ Hz, $h_{ac} = 12$ Oe. At $H_{dc} = 0.025$ T, $d\chi'(T)/dT$ exhibits one peak corresponding to the peak temperature T_{irr} of χ'' . Above $H_{dc} = 0.3$ T the second small peak in $\chi''(T)$ starts to develop becoming more pronounced with increasing H_{dc} . We observe that at this same temperature $d\chi'(T)/dT$ displays a minimum. The same plot for $h_{ac} = 1$ Oe is also shown in Figs. 5(e)–5(h). It is relevant to note that $d\chi'(T)/dT$ also exhibits a minimum above the threshold H_{thr} , although no second peak is observed on $\chi''(T)$ up to $H_{dc} = 8$ T. The appearance of the anomalous dip on $d\chi'(T)/dT$ in the PE region gives a strong indication that T_{p2} might be an intrinsic property of the PE. On the other hand, $T_{onset} (< T_{p2})$, which marks a crossover towards strong pinning, does depend on h_{ac} . If it is closely related to the PE, it would be natural to expect that T_{peak} will also be affected by h_{ac} . However, T_{peak} (and T_{p2}) remains almost unchanged with h_{ac} (Fig. 4), suggesting that the enhanced pinning does not produce any PE. This is reminiscent with the recent report on NbSe_2 ,³⁹ where an excess pinning associated with the crossover from weak to strong pinning is also found not to produce any PE. This scenario is in agreement with the collective pinning model according to which the softening of the elastic moduli results in the PE.⁴⁰ However, $\text{Ba}_{0.5}\text{K}_{0.5}\text{Fe}_2\text{As}_2$ single crystals display very strong pinning. Consequently, it does not seem plausible that the PE results only from weak collective pinning. In optimally doped $\text{Ba}_{0.5}\text{K}_{0.5}\text{Fe}_2\text{As}_2$ single crystals, the low density of twin boundaries cannot account for its strong pinning and we can discard them as the source of the peak effect.⁴¹ Specifically, $J_c(H, \theta)$ measurements on $\text{Ba}_{0.5}\text{K}_{0.5}\text{Fe}_2\text{As}_2$ single crystals have revealed no trace of extended defects playing the role of pinning centers,³² and scaling analysis have revealed that the strong pinning must arise as a consequence of isotropic pointlike defects. Indeed, it has been suggested that in this material, K doping introduces imperfections into the crystal lattice (due to its different ionic size compared to Ba^{2+})¹⁰ which act as intrinsic isotropic pinning centers. We argue that at T_{p2} a softening of the vortex lattice occurs which assists (and further enhances) the PE with increasing temperature. Yet, the major contribution to the PE arises from the order-disorder transition from a weak collective three-dimensional (3D)

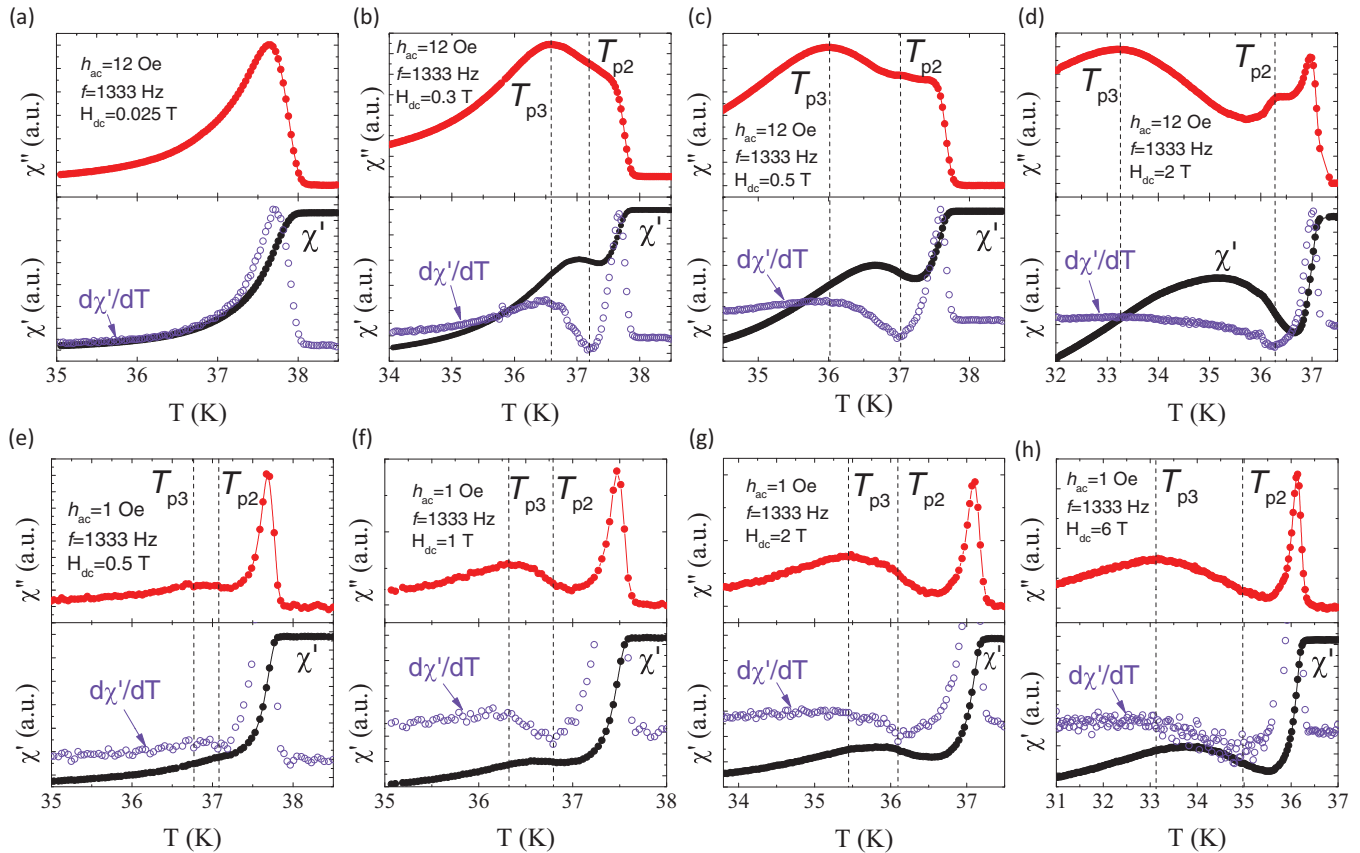


FIG. 5. (Color online) Temperature dependence of ac susceptibility for various dc fields at $f = 1333$ Hz, $h_{ac} = 12$ Oe (a)–(d) and $h_{ac} = 1$ Oe (e)–(h). The derivative $d\chi'/dT$ is also shown by the open circles in each panel. The dashed lines indicate the position of T_{p2} and T_{p3} .

pinning to a strong pinning scenario. Within this isotropic pinning landscape, one reasonable possibility is that the high temperature strong pinning regime appears due to a transition towards a one-dimensional (1D) collectively pinned vortex lattice.^{41,42}

The phase diagram presented in Fig. 6 shows a summary of the different characteristic temperatures determined from the $\chi'(T, H)$ and $\chi''(T, H)$ curves. At low temperatures the vortex lattice is found to be a weakly pinned ordered Bragg glass, at T_{onset} the disordered state percolates and J_c increases gradually. We have observed that T_{onset} shifts to the low temperature regime with increasing h_{ac} as indicated by the dashed arrow in Fig. 6. This can be explained by the enhancement of the penetration of the Meissner currents as h_{ac} increases. Slightly below T_{peak} , T_{p2} marks the development of a peak arising from the softening of the vortex lattice. At T_{peak} the vortex lattice (assisted by the softening occurring at T_{p2}) enters a 1D collective pinning regime reaching the most disordered state, hence J_c reaches the maximum. Within our experimental range, both T_{peak} and T_{p2} are nearly independent of h_{ac} , which supports the idea that there exists an intrinsic connection between them. Above T_{peak} , the vortex lattice experiences a first-order transition where thermal fluctuations become dominant and vortices are getting unpinned,³⁹ therefore, J_c decreases dramatically. We notice that the phase boundary of T_{peak} deduced from the present work is much closer to H_{c2} as compared with the boundary of SMP from the isothermal magnetization measurements in a similar single

crystal.²¹ Additionally, the fit of the experimental data using the empirical formula $H_{peak}(T) = H(0)[1 - T/T_c]^n$ yields

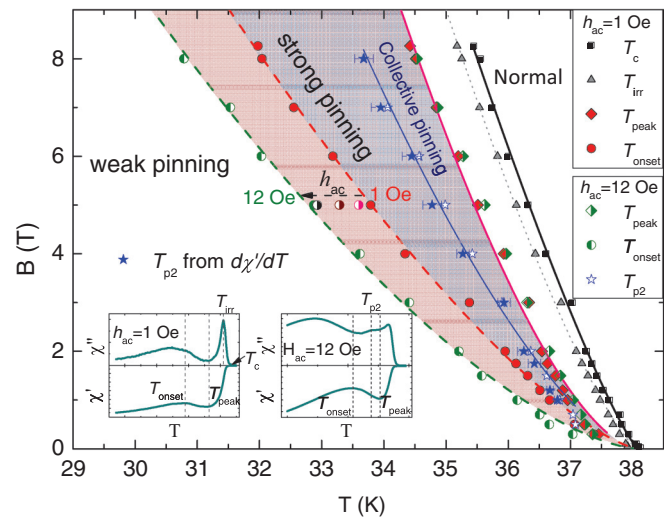


FIG. 6. (Color online) Phase diagram of vortex matter in $Ba_{0.5}K_{0.5}Fe_2As_2$ single crystal with $H \parallel c$. The shaded area between two dashed lines shows the enhanced pinning region with increasing h_{ac} as indicated by the arrow. The solid and dashed lines are plots using the empirical formula $H(T) = H(0)[1 - T/T_c]^n$ yielding $n = 1.31, 1.52,$ and 1.66 for $T_{irr}, T_{onset},$ and T_{peak} , respectively. The insets are the schematic ac susceptibility at $h_{ac} = 1$ and 12 Oe, showing the definition of the characteristic temperatures.

1.66 instead of $3/2$.²¹ These may indicate that the PE and SMP are induced by different mechanisms.

IV. SUMMARY

In summary, we report the observation of the peak effect in an iron-based superconductor $\text{Ba}_{0.5}\text{K}_{0.5}\text{Fe}_2\text{As}_2$ through the ac susceptibility measurements. The peak effect is found to display a strong history effect which can be explained by the competition between low temperature spontaneous ordering and the strong intrinsic pinning. An enhanced pinning region is observed with increasing h_{ac} , which is found not to produce any PE. Instead, an anomalous dissipation peak at T_{p2} , located well below T_{peak} on the phase diagram, is observed on $d\chi'(T)/dT$ curve at both low and high ac fields. Both T_{p2} and T_{peak} are found to be independent with h_{ac} . All the results suggest a close connection between T_{p2} and the peak effect. We suggest that the peak effect arises from the order-disorder transition of the vortex lattice (weak 3D to

strong 1D pinning), while the collective pinning related to the softening of the vortex lattice at T_{p2} further enhances the peak effect. Nevertheless, more studies are needed in order to fully clarify the origin of the peak effect in the 122 phase, as well as in other iron-based superconductors like the 1111 and the 11 phase.

ACKNOWLEDGMENTS

The work at KU Leuven is supported by the FWO, the Methusalem Funding by the Flemish Government, and the MR1201 COST Action. The work at Japan is financially supported by the World Premier International Research Center from MEXT, the Grants-in-Aid for Scientific Research from JSPS Japan, the Funding Program for World-Leading Innovative R&D on Science and Technology (FIRST Program) from JSPS, the Advanced Low Carbon Technology Research and Development Program (ALCA) from JST, and the National Natural Science Foundation of China (No.11234006).

*Junyi.Ge@fys.kuleuven.be

- ¹W. De Sorbo, *Rev. Mod. Phys.* **36**, 90 (1964).
- ²X. S. Ling, S. R. Park, B. A. McClain, S. M. Choi, D. C. Dender, and J. W. Lynn, *Phys. Rev. Lett.* **86**, 712 (2001).
- ³A. M. Troyanovski, M. van Hecke, N. Saha, J. Aarts, and P. H. Kes, *Phys. Rev. Lett.* **89**, 147006 (2002).
- ⁴I. K. Dimitrov, N. D. Daniilidis, C. Elbaum, J. W. Lynn, and X. S. Ling, *Phys. Rev. Lett.* **99**, 047001 (2007).
- ⁵M. Iavarone, R. Di Capua, G. Karapetrov, A. E. Koshelev, D. Rosenmann, H. Claus, C. D. Malliakas, M. G. Kanatzidis, T. Nishizaki, and N. Kobayashi, *Phys. Rev. B* **78**, 174518 (2008).
- ⁶Y. Kamihara, T. Watanabe, M. Hirano, and H. Hosono, *J. Am. Chem. Soc.* **130**, 3296 (2008).
- ⁷F. Hunte, J. Jaroszynski, A. Gurevich, D. C. Larbalesier, R. Jin, A. S. Sefat, M. A. McGuire, B. C. Sales, D. K. Christen, and D. Mandrus, *Nature (London)* **453**, 903 (2008).
- ⁸H. Q. Yuan, J. Singleton, F. F. Balakirev, S. A. Baily, G. F. Chen, J. L. Luo, and N. L. Wang, *Nature (London)* **457**, 565 (2009).
- ⁹K. Kadowaki, H. Takeya, and K. Hirata, *Phys. Rev. B* **54**, 462 (1996).
- ¹⁰X. L. Wang, S. R. Ghorbani, S. I. Lee, S. X. Dou, C. T. Lin, T. H. Johansen, K. H. Muller, Z. X. Cheng, G. Peleckis, M. Shabazi, A. J. Qviller, V. V. Yurchenko, G. L. Sun, and D. L. Sun, *Phys. Rev. B* **82**, 024525 (2010).
- ¹¹L. J. Li, T. Nishio, Z. A. Xu, and V. V. Moshchalkov, *Phys. Rev. B* **83**, 224522 (2011).
- ¹²H. Yang, B. Shen, Z. Wang, L. Shan, C. Ren, and H.-H. Wen, *Phys. Rev. B* **85**, 014524 (2012).
- ¹³Y. Yin, M. Zech, T. L. Williams, X. F. Wang, G. Wu, X. H. Chen, and J. E. Hoffman, *Phys. Rev. Lett.* **102**, 097002 (2009).
- ¹⁴T. Hanaguri, K. Kitagawa, K. Matsubayashi, Y. Mazaki, Y. Uwatoko, and H. Takagi, *Phys. Rev. B* **85**, 214505 (2012).
- ¹⁵L. Ya. Vinnikov, A. V. Radaev, I. S. Veshchunov, A. G. Troshina, Y. Liu, C. T. Lin, and A. V. Boris, *JETP Lett.* **93**, 287 (2011).
- ¹⁶A. D. Thakur, S. S. Banerjee, M. J. Higgins, S. Ramakrishnan, and A. K. Grover, *Phys. Rev. B* **72**, 134524 (2005).
- ¹⁷A. Crisan, A. Iyo, and Y. Tanaka, *Appl. Phys. Lett.* **83**, 506 (2003).
- ¹⁸P. Fabbriatore, S. Farinon, G. Gemme, R. Musenich, R. Parodi, and B. Zhang, *Phys. Rev. B* **50**, 3189 (1994).
- ¹⁹S. Y. Ding, G. Q. Wang, X. X. Yao, H. T. Peng, Q. Y. Peng, and S. H. Zhou, *Phys. Rev. B* **51**, 9107 (1995).
- ²⁰G. Blatter, M. N. Feigelman, V. B. Geschkenbein, A. I. Larkin, and V. M. Vinokur, *Rev. Mod. Phys.* **66**, 1125 (1994).
- ²¹H. Yang, H. Luo, Z. Wang, and H. H. Wen, *Appl. Phys. Lett.* **93**, 142506 (2008).
- ²²Q. P. Ding, Y. Tsuchiya, S. Mohan, T. Taen, Y. Nakajima, and T. Tamegai, *Phys. Rev. B* **85**, 104512 (2012).
- ²³J. Li, Y. F. Guo, S. B. Zhang, J. Yuan, Y. Tsujimoto, X. Wang, C. I. Sathish, Y. Sun, S. Yu, W. Yi, K. Yamaura, E. Takayama-Muromachiu, Y. Shirako, M. Akaogi, and H. Kontani, *Phys. Rev. B* **85**, 214509 (2012).
- ²⁴A. P. Malozemoff, T. K. Worthington, Y. Yeshurun, F. Holtzberg, and P. H. Kes, *Phys. Rev. B* **38**, 7203(R) (1988).
- ²⁵G. Prando, P. Carretta, R. De Renzi, S. Sanna, A. Palenzona, M. Putti, and M. Tropeano, *Phys. Rev. B* **83**, 174514 (2011).
- ²⁶T. Ishida, K. Okuda, and H. Asaoka, *Phys. Rev. B* **56**, 5128 (1997).
- ²⁷G. Pasquini, D. P. Daroca, C. Chilotte, G. S. Lozano, and V. Bekeris, *Phys. Rev. Lett.* **100**, 247003 (2008).
- ²⁸M. Pissas, S. Lee, A. Yamamoto, and S. Tajima, *Phys. Rev. Lett.* **89**, 097002 (2002).
- ²⁹S. R. Park, S. M. Choi, D. C. Dender, J. W. Lynn, and X. S. Ling, *Phys. Rev. Lett.* **91**, 167003 (2003).
- ³⁰Y. Paltiel, E. Zeldov, Y. N. Myasoedov, H. Shtrikman, S. Bhattacharya, M. J. Higgins, Z. L. Xiao, E. Y. Andrei, P. L. Gammel, and D. J. Bishop, *Nature (London)* **403**, 398 (2000).
- ³¹S. O. Valenzuela and V. Bekeris, *Phys. Rev. Lett.* **84**, 4200 (2000).
- ³²J. Li, J. Yuan, Y. H. Yuan, J. Ge, M. Y. Li, H. L. Feng, P. J. Pereira, A. Ishii, T. Hatano, A. V. Silhanek, L. F. Chibotaru, J. Vanacken, K. Yamaura, H. B. Wang, E. Takayama-Muromachi, and V. V. Moshchalkov, *Appl. Phys. Lett.* **103**, 062603 (2013).
- ³³C. P. Bean, *Phys. Rev. Lett.* **8**, 250 (1962).

- ³⁴S. L. Liu, G. J. Wu, X. B. Xu, J. Wu, H. M. Shao, Y. M. Cai, and X. C. Jin, *Phys. Lett. A* **339**, 408 (2005).
- ³⁵M. Andersson, A. Rydh, and O. Rapp, *Phys. Rev. B* **63**, 184511 (2001).
- ³⁶K. H. Fischer, *Supercond. Rev.* **1**, 153 (1995).
- ³⁷M. W. Lee, M. F. Tai, and J. B. Shi, *Physica C* **272**, 137 (1996).
- ³⁸Th. Herzog, H. A. Radovan, P. Ziemann, and E. H. Brandt, *Phys. Rev. B* **56**, 2871 (1997).
- ³⁹S. Mohan, J. Sinha, S. S. Banerjee, and Y. Myasoedov, *Phys. Rev. Lett.* **98**, 027003 (2007).
- ⁴⁰A. I. Larkin and Yu. N. Ovchinnikov, *J. Low Temp. Phys.* **34**, 409 (1979).
- ⁴¹A. I. Larkin, M. C. Marchetti, and V. M. Vinokur, *Phys. Rev. Lett.* **75**, 2992 (1995).
- ⁴²G. Blatter, V. B. Geshkenbein, and J. A. G. Koopmann, *Phys. Rev. Lett.* **92**, 067009 (2004).